Online estimation of atmospheric turbulence parameters and outer-scale profiling

Guesalaga, A., Neichel, B., Correia, C., Butterley, T., Osborn, J., et al.

A. Guesalaga, B. Neichel, C. Correia, T. Butterley, J. Osborn, E. Masciadri, T. Fusco, J.-F. Sauvage, "Online estimation of atmospheric turbulence parameters and outer-scale profiling," Proc. SPIE 9909, Adaptive Optics Systems V, 99093C (27 July 2016); doi: 10.1117/12.2231970

SPIE.

Event: SPIE Astronomical Telescopes + Instrumentation, 2016, Edinburgh, United Kingdom

On-line estimation of atmospheric turbulence parameters and outer-scale profiling

A.Guesalaga[*,1], B.Neichel[2], C.Correia[2], T.Butterley[3], J.Osborn[3], E.Masciadri[4], T.Fusco[2,5], J.-F.Sauvage[2,5]

[1]Pontificia Universidad Católica de Chile, 4860 Vicuña Mackenna, 7820436 Santiago, Chile
[2]Laboratoire d'Astrophysique de Marseille, Aix Marseille Université,, 13388 Marseille, France
[3]Durham University, South Road, Durham, DH1 3LE, United Kingdom
[4]INAF - Arcetri Astrophysical Observatory, Largo E. Fermi 5, I-50125 Firenze, Italy
[5]ONERA - 29 avenue de la Division Leclerc, F-92322 Chatillon Cedex, France

ABSTRACT

Estimating the outer scale profile, $\mathcal{L}_0(h)$ in the context of current very large and future extremely large telescopes is crucial, as it impacts the on-line estimation of turbulence parameters ($Cn^2(h)$, r_0, θ_0 and τ_0) and the performance of Wide Field Adaptive Optics (WFAO) systems. We describe an on-line technique that estimates $\mathcal{L}_0(h)$ using AO loop data available at the facility instruments. It constructs the cross-correlation functions of the slopes of two or more wavefront sensors, which are fitted to linear combinations of theoretical responses for individual layers with different altitudes and outer scale values.

We analyze some restrictions found in the estimation process, which are general to any measurement technique. The insensitivity of the instrument to large values of outer scale is one of them, as the telescope becomes blind to outer scales larger than its diameter. Another problem is the contradiction between the length of data and the stationarity assumption of the turbulence (turbulence parameters may change during the data acquisition time).

Our method effectively deals with problems such as noise estimation, asymmetric correlation functions and wavefront propagation effects. It is shown that the latter cannot be neglected in high resolution AO systems or strong turbulence at high altitudes. The method is applied to the Gemini South MCAO system (GeMS) that comprises five wavefront sensors and two DMs. Statistical values of $\mathcal{L}_0(h)$ at Cerro Pachón from data acquired with GeMS during three years are shown, where some interesting resemblance to other independent results in the literature are shown.

1. INTRODUCTION

Existing work on $\mathcal{L}_0$ estimation have shown that strong disagreements on the way it is estimated, the results, and its importance in AO areas such as PSF-R, tomography and turbulence profiling. One common approach to estimate the outer scale ($\mathcal{L}_0$) is to assume it as a global parameter and some work has been done towards developing models for its behaviour in altitude, i.e. $\mathcal{L}_0(h)$ [1,2].

In this article, we intend to contribute to the knowledge about this parameter by analysing a significant amount of data collected at the Gemini South MCAO system (GeMS) [3] during three years of campaigns and also developing a technique to estimate the outer scale profile, $\mathcal{L}_0(h)$.

1.1 Estimating the global $\mathcal{L}_0(h)$

A possible approach to estimate the global outer scale is to compute the autocorrelation of slopes using WFS data from atmosphere probing. The shape of these reference functions are related to the outer scale of the turbulence beneath the sodium layer.

A problem with this approach, common to any optical system with pupils (baselines) significantly smaller than the largest turbulence eddy, is that the techniques are not sensitive to them (see Fig. 1). Here, autocorrelation cuts are plotted for different outer scale values, that is: $\mathcal{L}_0 = \{1, 5, 10, 20, 30, 40, 50\}$ m. Notice that for large values of $\mathcal{L}_0$, the function become asymptotically the same. The rule of thumb is that a system is capable of correctly estimating $\mathcal{L}_0$s for sizes no larger than three to four times the size of the pupil or baseline.

*aguesala@ing.puc.cl

Adaptive Optics Systems V, edited by Enrico Marchetti, Laird M. Close, Jean-Pierre Véran, Proc. of SPIE Vol. 9909, 99093C

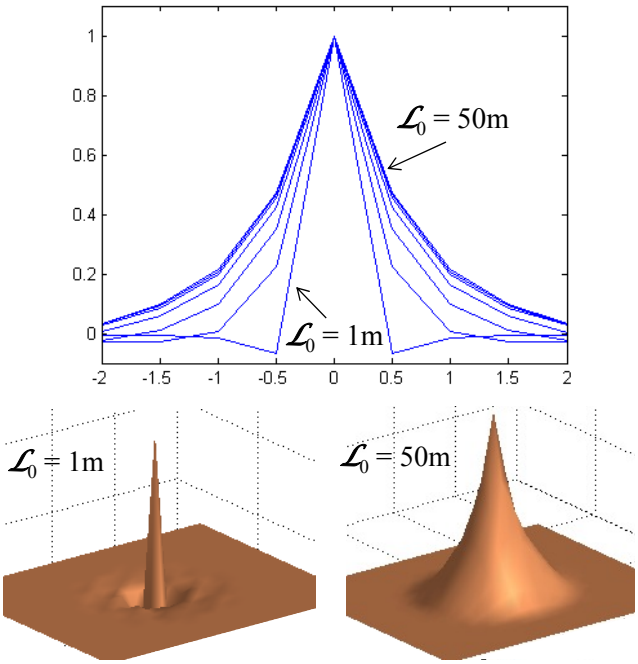

Figure 1. Simulated response functions (autocorrelations of slopes) for GeMS. Top: slices of normalized responses for $\mathcal{L}_0$ = {1, 5, 10, 20, 30, 40, 50} m. Bottom: 3D representation of response function for outer scales of 1 and 50m.

Furthermore, we have found that in the strict sense, there is no such thing as a "global" outer scale, since the response function is the result of combining slopes from two or more layers with not necessarily the same $\mathcal{L}_0$, i.e. a profile or $\mathcal{L}_0(h)$. This is not novel as previous reports and models have already identified this turbulence feature [1,2,4,5].

Figure 2 illustrates this turbulence feature by presenting two common cases found in responses from GeMS telemetry data. The first one (top) is a nearly single-mode response that can be represented by a single theoretical autocorrelation function. The second (bottom) is a more complex response where no single outer scale can represent it. In fact, by using fitting techniques, the most likely situation is that the response from the on-sky data is the result of at least two functions, each with its own outer scale, i.e. a two-mode response. Later in the article, we will see that this example is even richer in terms of the number of layers than can constitute it.

The complexity that arises when trying to identify the different outer scale components in the atmospheric volume is common to any technique based on optical instruments, such as 1D or 2D SLODAR-based sensors [6] or other based solely on tip-tilt measurements [1].

1.2 Estimation of noise in slopes

Furthermore, an additional problem appears in autocorrelation methods when trying to estimate the noise out of the responses (see Fig.2 below), which is a crucial step in the response fitting.

Spatial noise matches perfectly in autocorrelation maps, generating peaks that would generate an under-estimation of the outer scales, i.e. extremely narrow responses (those corresponding to small $\mathcal{L}_0$ values) become similar to noise autocorrelations. Hence, a reliable method of noise estimation is necessary in order to extract its distorting effects on the fitting of responses based on the autocorrelation of slopes. This is the case in methods that fit theoretical autocorrelation functions to those from on-sky data that generally leave out the central correlation map component (see Fig. 3). Unfortunately, we have found that unacceptable errors can occur when the probed turbulence is constructed out of more than one layer with different outer scales. This is clearly the 2-mode case in Fig.2.

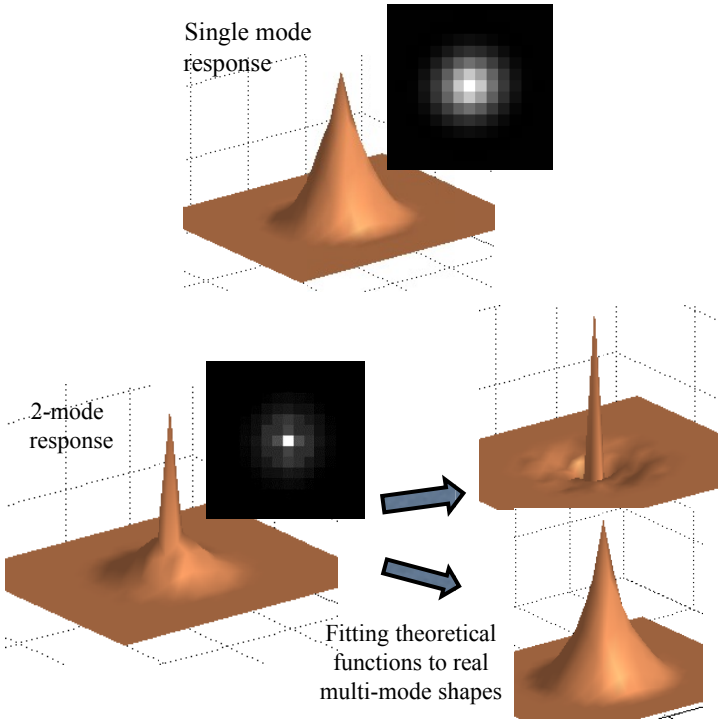

Figure 2. Response functions (autocorrelations of slopes) for GeMS from telemetry data. Top: single mode function (Feb 13, 2014, 04:56:16); Bottom: two-mode function (Apr 18, 2013, 06:05:50)

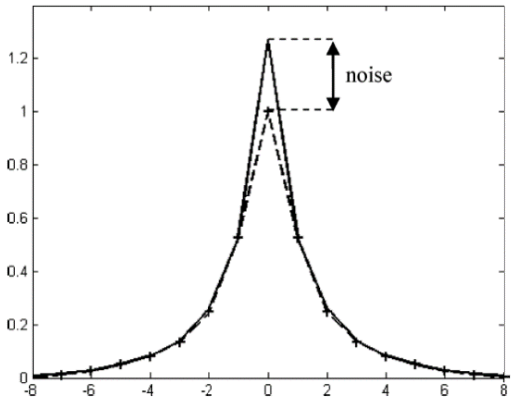

Figure 3. Fitting measured and theoretical responses for noise estimation (continuous line: on-sky data; dotted line: theoretical function)

Other possible approaches to estimate the noise level are:

- Analyzing PSDs of AO residual slopes at the higher end of the spectrum, where noise dominates. The weakness here is that vibration peaks and turbulence components from fast winds can contaminate this segment of the spectrum, generating significant errors in the estimation.
- Correlation of slopes from the same WFS but with a 1-frame delay, assuming that no temporal correlation of noise exists between successive frames (see Fig. 4). In our experience, this is by far the most reliable an accurate method, as long as both or either of the following conditions hold: high frame rates or low wind speeds. In other words, the product of frame rate times wind speed must be substantially smaller than the size of

the subaperture diameter. For GeMS operating at 500Hz with a wind of 20m/s, this product is 0.04m, much smaller that the subaperture diameter of 0.5m. It must be bear in mind that the actual outer scale in this case is also a source of error, but as long as it remains well above the subaperture diameter, its effect will not be significant.

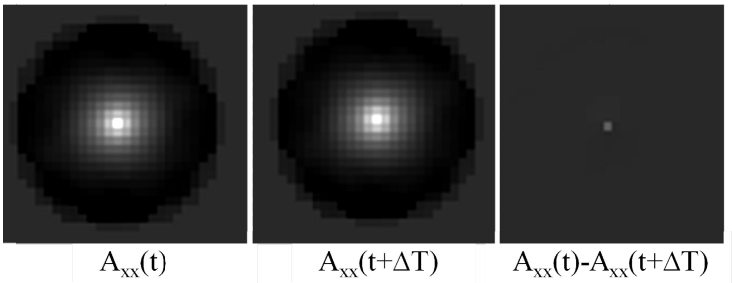

Figure 4. Autocorrelations between slopes from the same WFS and simultaneous data (left) and with one frame delay (center). The difference, assumed to be the noise component, is the difference of the two other images

1.3 The need for an outer scale profiler, $\mathcal{L}_0(h)$

The complexity of disentangling the different outer scales present in the turbulent layers probed by the telemetry system together with a lack of a reliable noise estimation method for all atmospheric and operational conditions, led us to discard the use of the autocorrelation approach. We now describe the method based on cross-correlations of the slopes from multiple WFS present in WFAO systems. In principle, this approach has two major advantages with respect to the previous method. Firstly, using different WFS, the detector noise problem does not exist. Second, by separating the turbulent layers in altitude by means of a C_n^2 profiler [7], the estimation of individual outer scales is a much more plausible problem.

The benefits of getting the distribution of the outer scale in altitude $\mathcal{L}_0(h)$ together with $C_n^2(h)$ allows us to better estimate atmospheric parameters such as: i) the global outer scale (spatial coherence) [8]; ii) seeing, in terms of the full width half maximum (FWHM) of the point spread function (PSF) [9,10]; iii) isoplanatic angle [10]; and iv) coherence time [10].

Since all these turbulence parameters depend on the outer scale stratification, It becomes clear that for WFAO systems and even the standard turbulence parameters, an outer scale profiler is a must. Next, we describe a technique to obtain this profile. It is meant to be embedded in a WFAO facility instruments such as GeMS or ESO's AOF [11], so it can provide better on-line turbulence information for operational purposes and also for site turbulence characterization.

2. A PROFILING METHOD FOR $\mathcal{L}_0(h)$

The method is based on the cross-correlation of telemetry data from multiple LGS WFSs. The result is a matrix corresponding to the impulse response of the telescope and atmospheric turbulence. The impulse response of the turbulence can be estimated by deconvolving the correlation functions of the slopes with the impulse function of the telescope, which gives the response of the atmospheric turbulence. The response of the turbulence is a function of the turbulence strength $C_n^2(h)$ and its spatial coherence $\mathcal{L}_0(h)$. By resolving an inverse problem, i.e. fitting individual theoretical responses for layers with different weights, altitudes and outer scales, the profile for the measured data for both $\mathcal{L}_0(h)$ and $C_n^2(h)$ can be simultaneously obtained.

Unfortunately, this inverse problem is not only a function of the spatial coherence given by $C_n^2(h)$ and $\mathcal{L}_0(h)$, but due to the telescope's aperture masking and Fresnel propagation effects it is also a function of the altitude of the layers. This makes an analytical approach extremely complex, as the response functions would be affected by so many factors that prevent to have a practical solution using this approach.

We have opted for a more practical approach, which is constructing -via simulation- a 2 dimensional array of the response functions for the possible values of $\mathcal{L}_0(h)$ and altitude h, which are subsequently combined to fit the measured correlations obtained from on-sky data. It becomes obvious that the spatial coherence $\mathcal{L}_0$ must be considered for the

generation of this basis (after normalizing for turbulence strength). Adding a second dimension corresponding to altitude is not that evident. The reasons why the basis for fitting has to be a function of altitude as well, are:

- Cross-correlation responses vary in altitude [6] and their asymmetry increases at higher altitudes. Also, the fratricide effect caused by sodium scattering in LGS (e,g, GeMS) generate further asymmetries even at the ground response function.
- It has also been shown [12,13] that propagation effects from higher layers are significant for subapertures diameters smaller than 0.2m. Errors as high as 30% are possible in the tip and tilt variances propagated from a layer at 10Km. In this case, the weak turbulence assumption does not hold and Fresnel propagation must be assumed. This effect also calls for a differentiation of correlation functions in altitude as the degree of diffraction will depend on the propagation distance. For GeMS (0.5m subaperture diameter), this effect is negligible.

Figure 5 shows two simulated response functions for a layer at the ground and at 10 Km using GeMS configuration parameters. Notice the difference in shape and asymmetry that can also vary over time due to effects such as dome seeing and, WFS dead detector pixels.

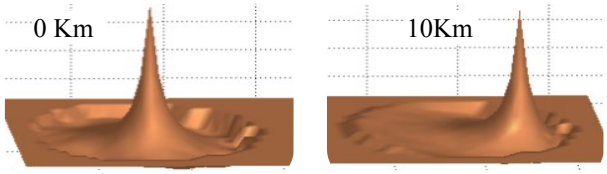

Figure 5. Simulated cross-correlation functions. Left: asymmetries at the ground due to fratricide masking; Right: asymmetry at higher altitude due to the finite nature of pupil and anisotropic overlapping.

It is obvious that trying to represent such behavior with analytical models would be extremely difficult, so in the next section we present our more practical approach that uses a limited number of response functions for different altitude and outer scales (mode basis) to solve this fitting problem.

2.1 The reference functions

The method consists in solving the inverse problem of identifying the parameters of each layer by fitting pre-calculated response functions to the one measured via telemetry. To do this, a two-dimensional array (mode basis) is constructed. It contains responses for N_H different altitudes and N_L different outer scale values. We call these "reference" functions C_{ref} ($\mathcal{L}_0$, h) and they are normalized to have the same $C_n^2(h)$ value. The figure below, simulated for GeMS, shows six cases for altitudes of 0, 5 and 10 Km and for outer scales of 2 and 50 meters. Notice that for higher altitudes, the position of the functions not only shifts along the baseline connecting two WFSs, but in the case of larger outer scales, it also changes in shape. Two differences are apparent: an asymmetry along the baseline and a sliding down a slope for the higher altitudes and larger $\mathcal{L}_0$. We think that the latter effects are more easily grabbed by simulated functions rather than trying to represent them by analytical functions.

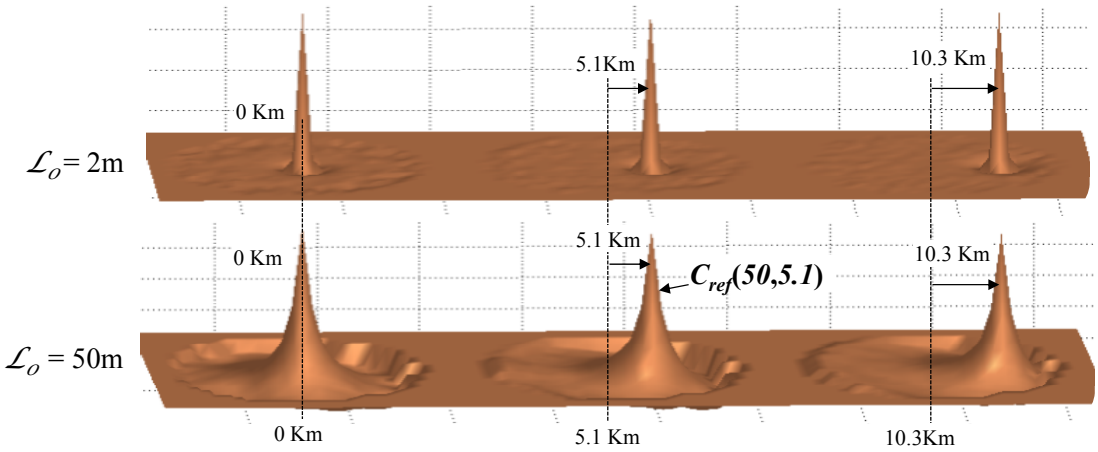

Figure 6. Simulated reference functions for three altitudes (horizontal) and two extreme values of outer scale (vertical)

2.2 Selection of altitudes and outer scales

For GeMS we choose altitude layers separated by 343.7 m, which is a fifth of the separation given by the subaperture diameter at the ground for the WFS combination that gives the best resolution in altitude [7]. In our case we have limited N_H to 50 layers, which gives a range between 0 and 17.2 Km.

The selection of outer scales is more complex. As shown in Fig. 7, the change in the response of the reference functions substantially decreases as they get larger. Notice that for values near 50 m the broadening is marginal. This suggests that an array of reference functions corresponding to a logarithmic distribution of $\mathcal{L}_0$ give a better representation of the changes for a limited number of these functions. For GeMS we have chosen $\mathcal{L}_0$: {1, 2, 3, 4, 6, 8, 11, 16, 22, 32, 50, 100}. Notice that even with a logarithmic distribution of $\mathcal{L}_0$, the curves still get closer together as one approaches the higher end of the range.

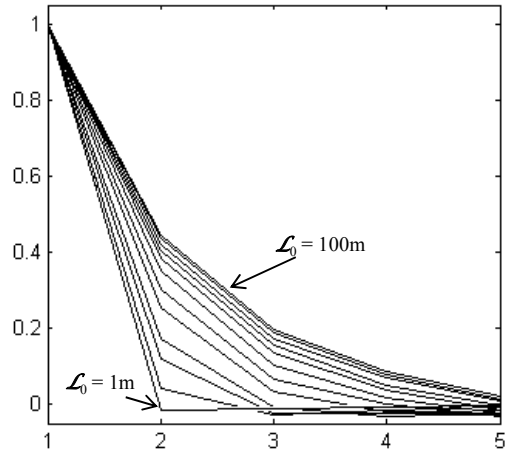

Figure 7. Cross section of reference functions for $\mathcal{L}_0$: {1, 2, 3, 4, 6, 8, 11, 16, 22, 32, 50, 100}. The difference in the shape are marginal in the higher end of the range

The array of discrete values for $\mathcal{L}_0$ and h would generate significant values in the fitting if the minimum were searched for only this set of functions. A first step considers the search of the best fit by scanning only these discrete values, however, a second stage in the optimization relaxes this restriction transforming the problem into a continuous one by looking for functions that are a linear combination of neighbors (interpolation). Figure 8 shows this process, where C_{ref} ($\mathcal{L}_0$, h) is calculated as:

$$C_{ref}(\mathcal{L}_0,h)=\Big((1-\alpha)\cdot C_{ref}(\mathcal{L}_0^i,h^j)+\alpha\cdot C_{ref}(\mathcal{L}_0^{i+1},h^j)\Big)\cdot(1-\beta)+\Big((1-\alpha)\cdot C_{ref}(\mathcal{L}_0^i,h^{j+1})+\alpha\cdot C_{ref}(\mathcal{L}_0^{i+1},h^{j+1})\Big)\cdot\beta \quad (1)$$

where α and β range are the weightings applied to the functions in the discrete grid defined in the [0, 1] range.

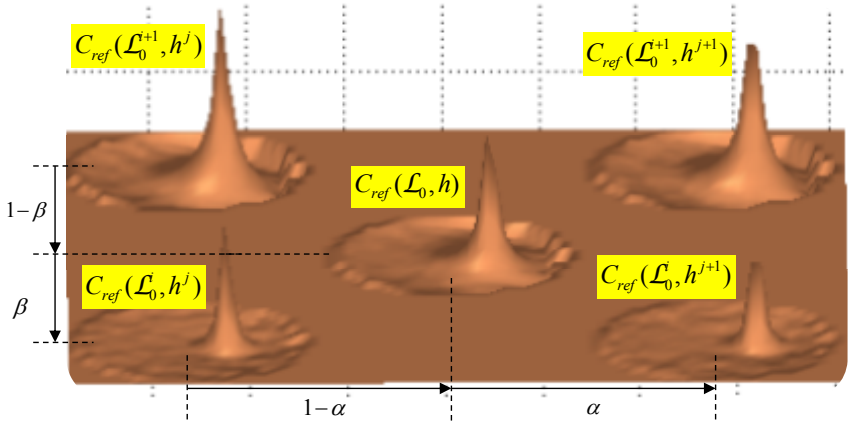

Figure 8. Interpolation of reference functions to transform the discrete search into a continuous one.

2.3 The fitting problem

The solution to the inverse problem can be mathematically expressed as the minimization of the fitting error given by:

$$\underset{\omega, \mathcal{L}_0, h}{Min} \left\langle \left(C_{meas} - \sum_{i=1}^{N_Z} \omega_i \cdot C_{ref}^i(\mathcal{L}_0, h) \right)^2 \right\rangle \qquad (2)$$

where C_{meas} is the correlation function computed from telemetry data and ω_i ($i = \{1, \ldots, N_Z\}$) are the weightings for each of the N_Z layers considered in the fitting. The choice of N_Z is given by the number of atmospheric layers that can be effectively estimated, given the number independent elements in C_{meas}. For GeMS we have found that $N_Z = 5$ represents the maximum number of distinguishable layers in the total set containing more than 1,000 samples, acquired during three years of campaigns.

In order to reduce the processing time, only a portion of the reference functions are used. Figure 9 shows the window where the fitting is carried out. Pixels outside this area either have no physical meaning (they correspond to extremely negative altitudes) or their signal to noise ratio is too low. The latter is caused by a small overlapping between different WFSs (very high altitudes). Notice that some pixels corresponding to negative altitude correlations are included in the area. This is because due to the turbulence spatial coherence, the convolved layer extends beyond a single pixel.

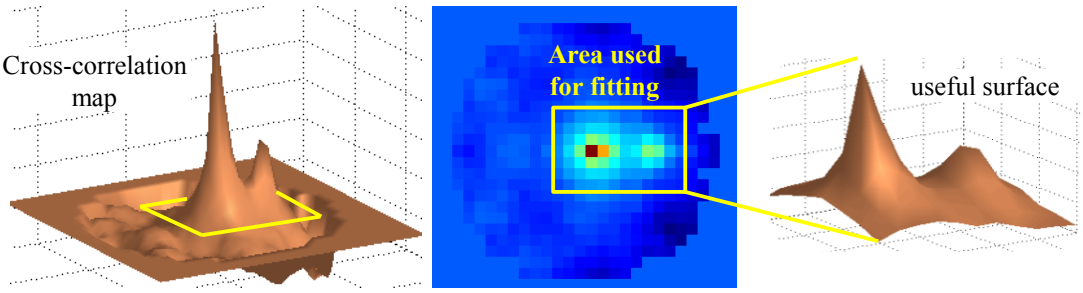

Figure 9. Area used for fitting (yellow window). On-sky data from May 22, 2013, 02:41:12

Once the correlation function of the measured slopes is constructed (C_{meas}), the search for the best fitting is carried out. Figure 10 illustrates this process.

Using a search algorithm known as trust-region-reflective [14,15] the best values for $\mathcal{L}_0$, h and ω are obtained. The values *of* α and β are respectively slaved to $\mathcal{L}_0$ and h. The optimization technique is particularly suited for this problem as it can handle the minimization of quadratic functions subject to bounds on some of the variables. In the case of ω, a

non-negativity restriction must be met. For h and $\mathcal{L}_0$, lower and upper bounds exist. The altitude spans from 0 Km to the maximum detectable range which is equivalent to the 17Km given by the overlapping of the WFS at high altitudes. For the outer scale, minimum and maximum values of 1 m and 100 m has been defined.

The measured response function (C_{meas}) is shown on the upper left panel. The fitting search looks for a combination of layers that fit this function. The upper-right panel shows the result of the search for $N_Z = 5$, where the fitting is separated in their basis constituents. The table lists the parameters found for every layer which when combined and subtracted to C_{meas} give the minimum fitting error defined by equation (6).

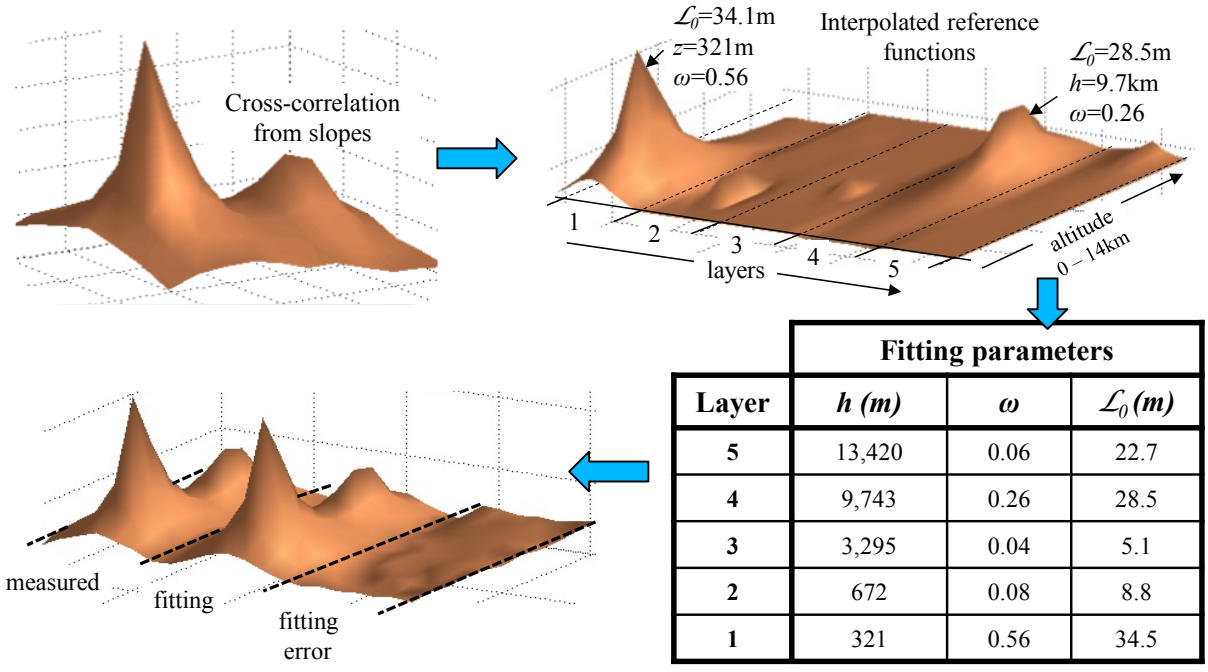

	Fitting parameters		
Layer	***h* (m)**	**ω**	**$\mathcal{L}_0$ (m)**
5	13,420	0.06	22.7
4	9,743	0.26	28.5
3	3,295	0.04	5.1
2	672	0.08	8.8
1	321	0.56	34.5

Figure 10. Fitting of reference function to measured cross-correlation function. On-sky data from May 22, 2013, 02:41:12

The table provides the turbulence profile via the weights (ω_i^*) of the 5 basis modes found. By knowing the values of $\mathcal{L}_0$ for each layer, more accurate atmosphere parameters ($C_n^2(h)$, θ_0, τ_0, r_0 and PSF-FWHM), can also be estimated.

The three surfaces in the bottom-left panel correspond to: i) the measured cross-correlation for the 4 possible baselines between the WFS at the corners of the LGS asterism (left); ii) the weighted sum of the 5 reference functions found in the fitting (center); and iii) the difference between the left and center surfaces (right).

2.4 Case with two extreme $\mathcal{L}_0$ values at the ground

An interesting case is when two layers with different outer scale values co-exist at very similar heights. This is the case for the profile shown in Fig. 12. A strong layer with 50m outer scale is merged with another having an outer scale of just 1m. Notice that this situation can be better seen in the autocorrelation function, where a shoulder in the skirt of the auto-correlation function appears.

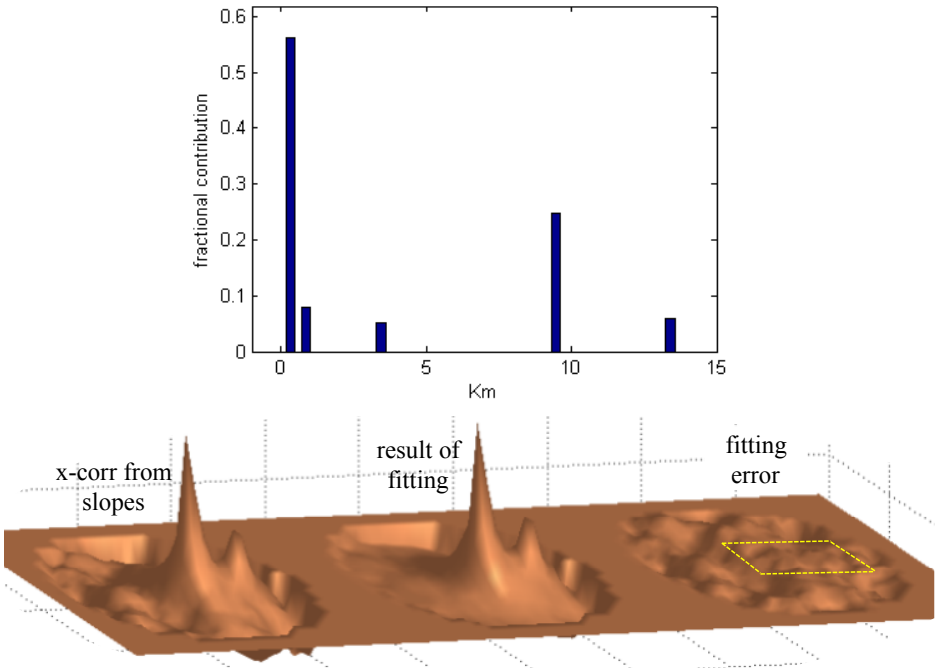

Figure 11. Top: turbulence profile for the case of study (fractional). Bottom: measured (left), fitted (center) and fitting error (right). The yellow box corresponds to the area used for fitting. On-sky data from May 22 2013, 02:41:12

The method works extremely well under these circumstances, with a clear distinction of both layers in the estimated profile.

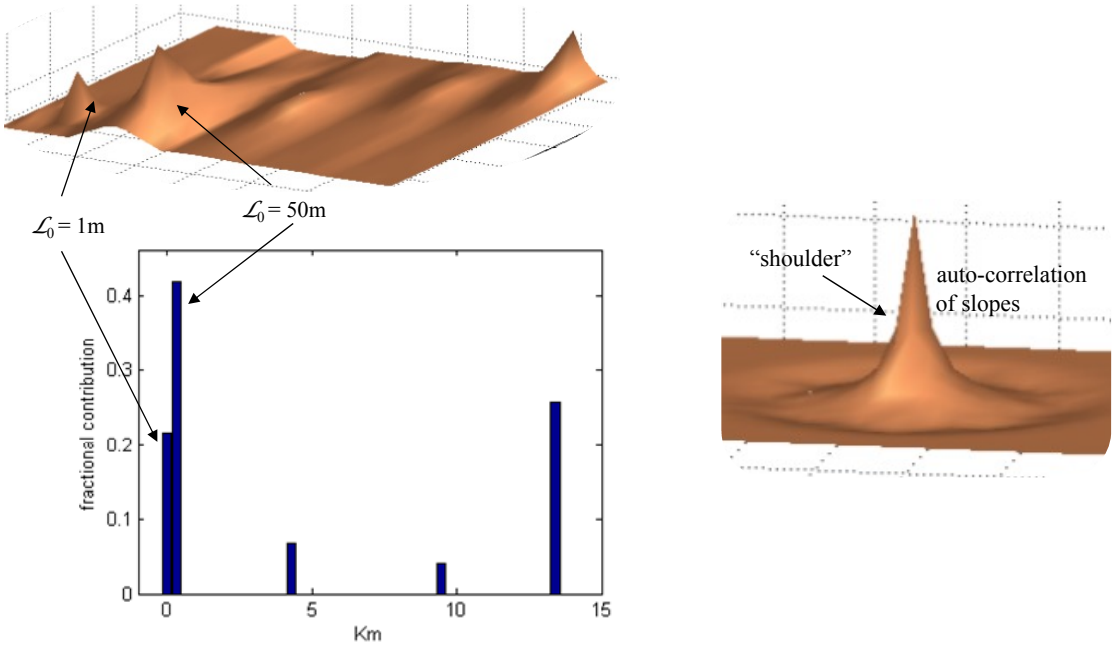

Figure 12. Case of two layers close to the ground with different outer scale values. The right panel shows the autocorrelation function where a shoulder suggesting the existence of more than one value of $\mathcal{L}_0$. On-sky data from Apr 18, 2013, 06:05:50.

3. RESULTS FOR $\mathcal{L}_0(h)$ FROM GeMS TELEMETRY

A significant amount of telemetry data collected with GeMS during three years of campaigns (2012 thru 2014) has been processed to estimate the profile of the outer scale, $\mathcal{L}_0(h)$. The results obtained for 1124 samples are presented in the Fig. 13, where the profile is divided in slabs of 2Km, except for the two divisions closer to the ground. The abundant data available in the first 2 Km allowed us to further divide this segment into two slabs 1Km each.

An average of 24.0 m and a median of 17.5 m were estimated for the complete set of samples. However, we think that these values are misleading and should not be used for two reasons: i) the estimation range has been limited at 50 m due to the telescope blindness for larger values of $\mathcal{L}_0$; ii) in many altitude segments, multimode histograms are found, make a single scalar parameter meaningless. For instance, the bar plot on the left (histogram of the first 1 Km slab), clearly detects at least two modes at both extremes (1m and 50m).

In any case, the profile has many characteristics common to other previously reported profiles obtained in independent campaigns [1,2], where the maximum values for $\mathcal{L}_0$ are obtained for altitudes between 1 and 2 Km and the smallest are located between 2 and 4 Km.

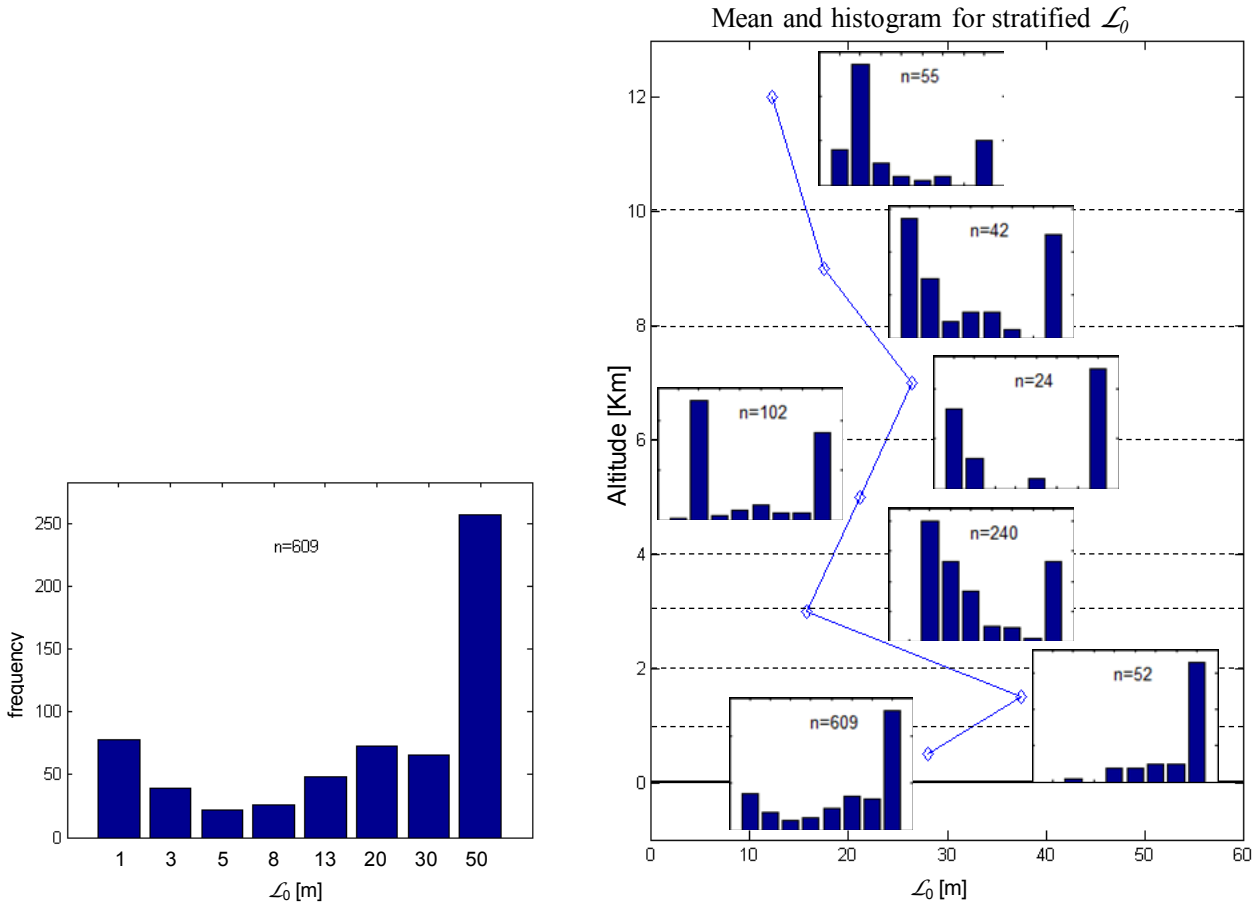

Figure 13. Profile of outer scale for the three years' data (right panel, diamonds). The profile has been divided in slabs of 1 and 2 Km, as shown in the right panel (thanks to the abundancy of data at lower heights). In many altitude segments, multimode histograms are detected. The bar plot on the left panel shows two modes at the extremes of the histogram range (1 and 50 meters) for the lowest segment.

4. CONCLUSIONS

Significant errors are found in the estimation of large values of $\mathcal{L}_0$, i.e. greater that the telescope diameter. However, as these estimations are meant to be used by the telescope instruments, the deviations from the real values are less relevant as the corrections cannot reach them either. Future giant telescopes will require a precise estimation of this parameter for larger outer scales ($\mathcal{L}_0 > 30$m), but their larger aperture and high resolution wavefront sensors will allow to increase the range of the accurately estimated values of $\mathcal{L}_0$.

Further work includes the error analysis of the method via simulation. In particular, we have found that having uncorrelated slopes (time-wise) to construct the correlation functions is a must, and decimation in the storage process seems a good solution to provide the profiler with temporally independent slopes in reasonable data chunks. It is obvious that the longer the data sequence the better for the accuracy of the profiler; however, it remains to be determined what is the longest sequence that can be processed without breaking the stationarity assumption of the turbulence statistics.

5. REFERENCES

[1] Ziad A., Blary F., Borgnino J. et al, PML/PBL: A new generalized monitor of atmospheric turbulence profiles, AO4ELT3 Conference, Florence, 2013

[2] Dali A., Ziad, A., Berdja, A., et al. (2010), Multi-instrument measurement campaign at Paranal in 2007. Characterization of the outer scale and the seeing of the surface layer, A&A, 524, A73

[3] Neichel B., Rigaut F., Bec M, The Gemini MCAO System GeMS: nearing the end of a lab-story, Proc. SPIE 7736, pp. 773606, 2010

[4] Coulman C. E., Vernin J., Coqueugniot Y., Caccia J. L. (1988) Outer scale of turbulence appropriate to modeling refractive-index structure profiles. Applied Optics 27, 155.

[5] Lukin, V. P., Fortes, Boris V. and Nosov, Evgenii V, Effective outer scale of turbulence for imaging through the atmosphere, Proc. SPIE, 3353 Adaptive Optical System Technologies, p. 1121-1129,1998

[6] Butterley, T., Wilson, R. W. and Sarazin, M. (2006), Determination of the profile of atmospheric optical turbulence strength from SLODAR data. MNRAS, 369: 835–845

[7] Cortés A., Neichel B., Guesalaga A., Osborn J., Rigaut F. and Guzmán D. (2012) Atmospheric turbulence profiling using multiple laser star wavefront sensors. Monthly Notices of the Royal Astronomical Society, 427, 3, 2089–2099

[8] Julien Borgnino, Estimation of the spatial coherence outer scale relevant to long baseline interferometry and imaging in optical astronomy, Appl. Opt. 29, 1863-1865 (1990)

[9] Tokovinin, A. (2002), From Differential Image Motion to Seeing, Publications of the Astronomical Society of the Pacific, PASP, 114, 1156-1166

[10] R. Conan, “Modelisation des effets de l’echelle externe de coherence spatiale du front d’onde pour l’observation a haute resolution angulaire en astronomie,” Ph.D. thesis (Université Nice Sophia Antipolis, 2000)

[11] Arsenault, R., Madec, P.Y., Paufique, J., et al., ESO AOF Progress Report, Proc. SPIE 8447, 0J (2012)

[12] Goodwin M., Jenkins C., and Lambert A., Improved detection of atmospheric turbulence with SLODAR, Opt. Express 15, 14844-14860 (2007)

[13] Tokovinin A. and Kornilov V., Accurate seeing measurements with MASS and DIMM, MNRAS, 381, pp.1179-1189, (2007)

[14] Moré, J.J. and D.C. Sorensen, Computing a Trust Region Step, SIAM Journal on Scientific and Statistical Computing, Vol. 3, pp 553–572, 1983.

[15] Coleman, T.F. and Y. Li, "A Reflective Newton Method for Minimizing a Quadratic Function Subject to Bounds on some of the Variables," SIAM Journal on Optimization, Vol. 6, Number 4, pp 1040–1058, 1996

[16] Conan R., Correia C., Object-oriented Matlab adaptive optics toolbox, Proc. SPIE 9148, Adaptive Optics Systems IV, 91486C, 2014

[17] Maire J., Ziad A., Borgnino J. and Martin F., Measurements of profiles of the wavefront outer scale using observations of the limb of the Moon, Mon. Not. R. Astron. Soc. 377, 1236–1244 (2007)

ACKNOWLEDGEMENTS

This project has been supported by Fondecyt, grant 1160236.